



# Effective depolymerization of alkali lignin into phenolic monomers over ZrP catalysts promoted by Ni and W

Dandan Wang<sup>1</sup> · Xinyu Lu<sup>1</sup> · Haoquan Guo<sup>1</sup> · Pengcheng Xiu<sup>1</sup> · Jiajia Chen<sup>1</sup> · Yu Qin<sup>1</sup> · Hossain Mahmud Robin<sup>1</sup> · Chaozhong Xu<sup>1</sup> · Xiaoli Gu<sup>1</sup>

Received: 21 February 2021 / Revised: 9 May 2021 / Accepted: 14 May 2021 / Published online: 25 May 2021  
© The Author(s), under exclusive licence to Springer-Verlag GmbH Germany, part of Springer Nature 2021

## Abstract

A large amount of alkali lignin by-product is produced by the pulp and paper industry which can be further processed and transformed into valuable chemicals. In this study, the catalyst Ni-W/ZrP was prepared via chemical reduction for catalyzing alkali lignin depolymerization. Effective conversion of alkali lignin to phenolic monomers with assistance of formic acid acted as an internal hydrogen donor was performed in isopropanol system from 180 to 240 °C. Effects of reaction temperature, catalyst loading, and formic acid addition on lignin conversion were all investigated. Results showed that the highest oil yield was obtained (74.66 wt%) at 240 °C. The presence of formic acid could enhance alkali lignin conversion (the yield of bio-oil ranged from 17 to 23 wt% at 220 °C when the reaction conditions were changed from no added formic acid to only added formic acid). According to the GC/MS analysis, when metal loading (the mass ratio of Ni and W is 1:1) was 20 wt% (based on ZrP input), the prepared catalyst (Ni-W)<sub>20</sub>/ZrP had best selectivity for the phenolic products (88.25%, relative content). Furthermore, the obtained catalyst had different catalytic selectivities to G-type phenols and vanillin at different temperatures (from 180 to 240 °C). The quantitative analysis of bio-oil showed that the four products with high content in bio-oil were phenol, 2-methoxy (1.21 wt%), phenol, 4-ethyl-2-methoxy (0.45 wt%), vanillin (4.09 wt%), and ethenone,1-(4-hydroxy-3-methoxy-henyl) (0.86 wt%). FTIR analysis showed that peaks at 1267 cm<sup>-1</sup>, 1213 cm<sup>-1</sup>, 1130 cm<sup>-1</sup>, and 1046 cm<sup>-1</sup> (C-O bonds in guaiac-based and clove-based units) gradually decrease with the increase of temperature which indicates that lignin is depolymerized to monoaromatic units effectively. Finally, the catalyst (Ni-W)<sub>20</sub>/ZrP can be recycled five times without significant activity loss, indicating that it was a promising catalyst for lignin depolymerization.

**Keywords** Alkali lignin · Depolymerization · Bio-oil · Phenolic monomers

## 1 Introduction

Lignin is the largest renewable resource of aromatic biopolymer on earth, accounting for 15–40% of dry weight of most

plants. However, it is often underutilized in biorefining and pulping processes and is considered a low-value by-product [1].

Lignin is mainly composed of three kinds of alcohol monomers (coniferyl, para-coumaryl, and sinapyl alcohol) through C-O-C bond (e.g.,  $\beta$ -O-4,  $\alpha$ -O-4, and 4-O-5) and C-C bond (e.g.,  $\beta$ -1,  $\beta$ - $\beta$ , and 5-5) formed a cross-linked phenolic polymer [2–4]. Moreover, it has various functional groups, such as hydroxyl and benzene, which make lignin have a high using value. Through depolymerization reactions, lignin can be converted into phenols, aliphatics, acids, etc. [1].

There are many ways to convert lignin into chemicals, such as gasification, pyrolysis [5, 6], liquefaction, hydrodeoxygenation [7–9], hydrolysis [10–12], hydrogenolysis [13–15], and oxidation [16–18]. Nowadays, as hydrolysis can lead to higher lignin conversion, catalytic selectivity, and production towards phenolic monomers, it is

**Highlights** • Efficient strategy was proposed for phenol production from alkali lignin.

- 74.66 wt% of bio-oil yield was obtained over (Ni-W)<sub>20</sub>/ZrP catalyst.
- The catalyst Ni-W/ZrP was effectively selective for G-phenols.

✉ Chaozhong Xu  
xucz@njfu.edu.cn

✉ Xiaoli Gu  
guxiaoli@njfu.edu.cn

<sup>1</sup> Co-Innovation Center for Efficient Processing and Utilization of Forest Products, College of Chemical Engineering, Nanjing Forestry University, 159 Longpan Road, Nanjing 210037, People's Republic of China

**Table 1** Elemental analysis of alkali lignin

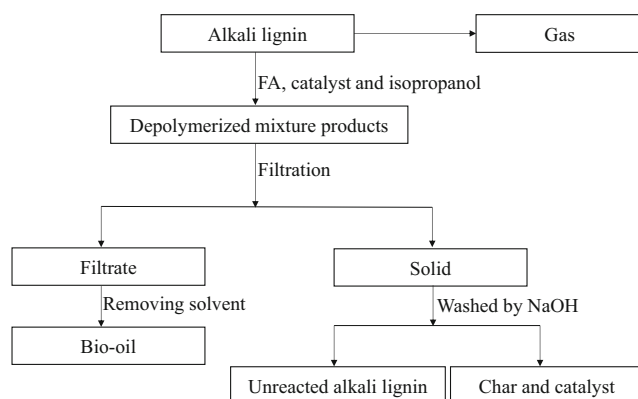
Sample	Carbon/ wt%	Nitrogen/ wt%	Hydrogen/ wt%	Oxygen/ wt% <sup>a</sup>
Lignin	42.96	5.23	5.48	46.33

<sup>a</sup> Calculate the oxygen content by difference

considered to be the most promising method [19]. In order to enhance the selective depolymerization of lignin, selecting an efficient and feasible catalyst is essential. Various noble metal-loaded catalysts (e.g., Pt/C, Pd/C, and Ru/C) were used in lignin-catalyzed hydrogenolysis [13, 20, 21]. However, due to the expensive price of noble metal-loaded catalysts, they do not meet the requirement of industrial production.

Moreover, it can lead to excessive hydrogenation of obtained products and increasing generation of char. Therefore, non-noble metal-loaded catalysts have become the hot researching spot for lignin hydrogenolysis, wherein Ni-, Mo-, and W-supported mesoporous catalysts are recognized as effective ones towards lignin hydrogenolysis [19, 22, 23]. Because these non-precious metals exhibit effective catalytic activity and selectivity in the catalytic conversion of lignin [24, 25]. For example, Song et al. [26] demonstrated that Ni/C showed effective catalytic activity and selectivity during the conversion of lignin into phenolic compounds (containing propylguaiacol, and propylsyringol). Meanwhile, Song et al. [27] used Co-Mo/ZrO<sub>2</sub> catalyst to catalyze lignin, and the yield of aromatic hydrocarbons was 21.9 wt%. Except for active metals, properties of support also play a key role in catalytic activity. For instance, zirconium phosphate (ZrP) is a layered solid catalyst containing abundant Lewis acid sites, which is demonstrated to be beneficial for lignin depolymerization [28, 29]; thus, it has been widely used as an efficient catalyst in biomass catalytic conversion [30, 31].

In this paper, a non-noble bimetallic catalyst Ni-W/ZrP was prepared via chemical reduction method using NaBH<sub>4</sub> as a reduction agent. The chemical and physical properties of prepared catalyst were studied by XRD, SEM-EDX, and BET.

**Fig. 1** Separation steps of depolymerization products of alkali lignin**Table 2** Composition of (Ni-W)<sub>20</sub>/ZrP catalyst

Element	wt%
P	33.12
Zr	47.87
Ni	9.89
W	9.11

Additionally, effects of reaction temperature (from 180 to 240 °C), metal loading (Ni and W, from 10 to 25 wt%, based on ZrP input), catalyst, and FA additions on the depolymerization of alkali lignin were all studied. For further figuring out the depolymerized mechanism, lignin-derived bio-oil and unreacted lignin were analyzed by various physicochemical characterizations including GC-MS and FTIR. At last, four experimental runs of catalyst were conducted for evaluating the catalyst recyclability.

## 2 Experimental section

### 2.1 Materials

Alkali lignin was purchased from TCI Development Co., Ltd. (Shanghai, China). **Table 1** shows the elemental analysis of alkali lignin.

Zirconyl chloride octahydrate (ZrOCl<sub>2</sub>·8H<sub>2</sub>O, AR, 98%), ammonium metatungstate ((NH<sub>4</sub>)<sub>6</sub>H<sub>2</sub>W<sub>12</sub>O<sub>40</sub>·xH<sub>2</sub>O, AR, 98%), nickel (II) nitrate hexahydrate (Ni(NO<sub>3</sub>)<sub>2</sub>·6H<sub>2</sub>O, AR, 98%), ammonium dihydrogen phosphate (H<sub>2</sub>NO<sub>4</sub>P, AR, 99%), sodium borohydride (NaBH<sub>4</sub>, AR, 90%), sodium hydroxide (NaOH, AR, 96%), formic acid (FA, AR, 85%), isopropanol (HPLC, ≥ 99.9%), ethanol (AR, 95%; HPLC, ≥ 99.8%), and dichloromethane (DCM, AR, 99%) were all purchased from Nanjing Chemical Reagent Co., Ltd. (Nanjing, China).

### 2.2 Catalyst preparation

Zirconium phosphate (ZrP) support was first prepared by deposition precipitation method; 140 mL NH<sub>4</sub>H<sub>2</sub>PO<sub>4</sub> solution (0.5 mol L<sup>-1</sup>) was added rapidly into 35 mL ZrOCl<sub>2</sub>·8H<sub>2</sub>O solution (1.0 mol L<sup>-1</sup>) in a three-necked flask. After 1 h stir, the obtained white precipitate was filtered, and centrifuged 3 times by washing with distilled water and dried at 100 °C. The resulting solid was ground (100–120 mesh). Finally, the ZrP support was obtained by calcined at 400 °C for 4 h with a heating rate of 5 °C/min in static air.

The preparation of a catalyst (Ni-W/ZrP) is by chemical reduction, and the reducing agent is NaBH<sub>4</sub>. The mass ratio of two metals was 1:1, and four different metal loadings (wt%, (Ni-W)<sub>x</sub>/ZrP, where x = 10, 15, 20, and 25 wt%) were

conducted as the following steps. Taking the synthesis of (Ni-W)<sub>10</sub>/ZrP as the example, 0.2477 g nickel (II) nitrate hexahydrate and 0.8089 g ammonium metatungstate hydrate were added into 30 mL deionized water and stirred for 30 min until dissolution. After 1 h of stirring, 1 g of the support was added into the metal precursor solution, and stirring was continued for 2 h. Then, excessive NaHB<sub>4</sub> was added to the previous solution and continued to stir for 2 h to complete the reduction. At last, (Ni-W)<sub>10</sub>/ZrP catalyst was obtained by filtration, washing with deionized water for 3 times, and drying at 100 °C for 24 h.

### 2.3 Catalyst characterization

The morphology and elemental composition of the prepared catalyst were determined by scanning electron microscope-energy dispersive x-ray spectroscopy (SEM-EDX). The phase transition and crystal structure of the synthesis catalyst were studied by powder x-ray diffraction (XRD) technology. The wavelength of Cu K $\alpha$  radiation was 1.54006 Å. The scan angle of 2 $\theta$  was measured from 10 to 80° at a scan rate of 0.05° s<sup>-1</sup>. The specific surface area, pore volume, and pore size of the catalyst were measured by Micromeritics 113 ASAP 2020 instrument. Set the liquid nitrogen temperature to 77 K (-196 °C) and degassed all samples under 150 °C N<sub>2</sub> atmosphere before the start of the adsorption process.

### 2.4 Depolymerization of lignin

The lignin depolymerization reaction was conducted in a 100 mL reaction kettle. Then, 0.5 g lignin, 0.2 g catalyst, 5 mL FA, and 50 mL isopropanol were charged into the stainless steel reactor. In the absence of external pressure, the stainless steel reactor was heated to the specified temperature (180–240 °C) for 8 h. After the reaction is completed, the reactor is put into ice water to quench the reaction.

Figure 1 shows the separation process of lignin depolymerization. The obtained products were divided into three components (gas, liquid, and solid phases), while the discussion on gas is ignored because of the relatively small amount of gas production (less than 0.5 wt%). According to the previous study [32], solid-liquid separation was performed by the suction filter and the char was washed with dichloromethane (50 mL  $\times$  3), and liquid products obtained were evaporated at 55 °C to remove solvent and DCM to obtain bio-oil. In order to recycle the catalyst used, the coke, catalyst, and unreacted lignin were dissolved in 0.025 mol L<sup>-1</sup> NaOH solution, and the resulting solid was used in the cycle experiment. The resulting liquid was acidified with HCl to obtain unreacted lignin. The remaining solid (used catalyst and char) was dried overnight at 105 °C for further test.

### 2.5 Product characterization

Vario EL III was used to analyze the content (wt%) of carbon (C), hydrogen (H), and nitrogen (N) in the CHN mode, and the difference method was used (100 wt% - (C wt% + N wt% + H wt%)) to carry out the content (wt%) of oxygen (O). The changes in the functional groups of the unreacted lignin were obtained by Fourier-transform infrared spectroscopy (FTIR) on a Vertex 70 spectrometer. The wavelength range is 4000–500 cm<sup>-1</sup> with 32 scans collected per spectrum and a resolution of 4 wavenumbers. The composition of bio-oil was analyzed by the Gas chromatography–mass spectrometer (GC-MS). Before analysis, all bio-oil samples were dissolved in ethanol (HPLC) to a uniform concentration of 50 mg mL<sup>-1</sup>. The heating start temperature was 50 °C, keep it for 1 min, then adjusted the heating rate to 8°Cmin<sup>-1</sup> and kept it for 1 min; the final temperature was 220 °C, finally adjusted the heating rate to 10 °C min<sup>-1</sup> and kept it for 1 min; and the final temperature was 300 °C. The gas chromatography-flame ionization detector (GC-FID) (Agilent 5975C) was used to quantitatively analyze bio-oil with acetophenone as the internal standard, and the program conditions are the same as GC-MS analysis.

Finally, the yields (wt%) of gas, char, bio-oil, unreacted lignin, and main phenolic products were figured up across Eq. (1–5).

$$\text{the yield of bio-oil (wt.\%)} = \frac{m_{\text{bio-oil}}}{m_{\text{alkalilignin}}} \quad (1)$$

$$\text{the yield of gas (wt.\%)} = \frac{m_{\text{difference}}}{m_{\text{alkalilignin}}} \times 100\% \quad (2)$$

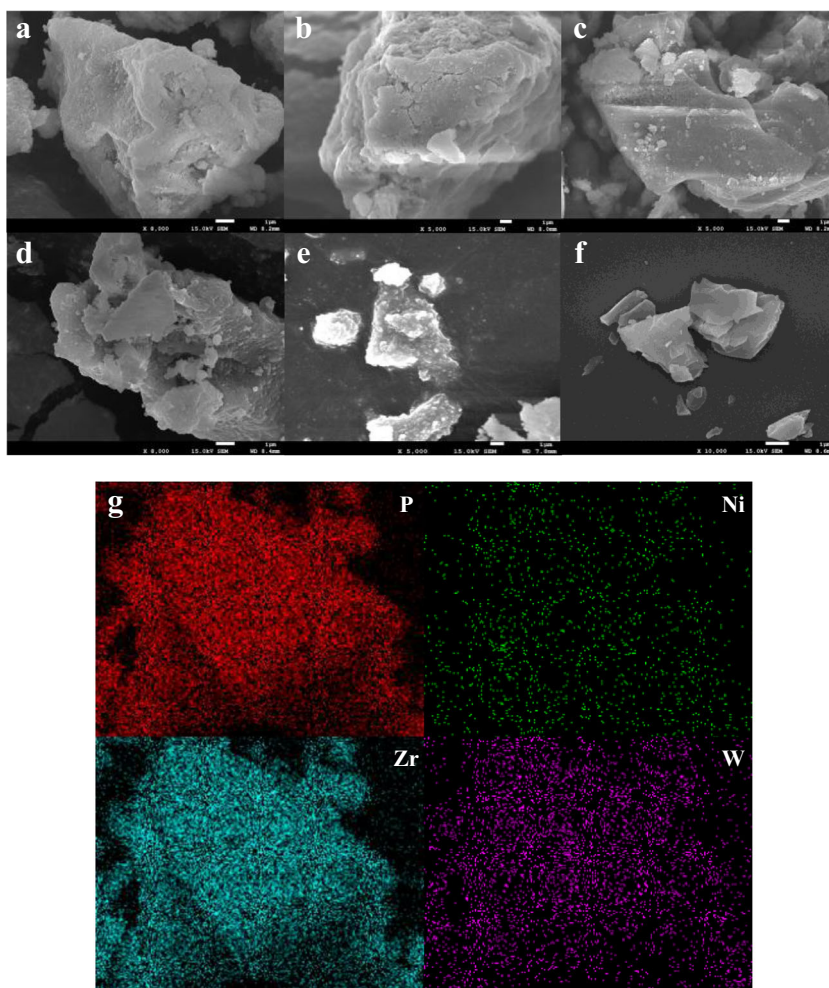
$$\begin{aligned} \text{the yield of unreacted alkali lignin (wt.\%)} \\ = \frac{m_{\text{unreactedalkalilignin}}}{m_{\text{alkalilignin}}} \times 100\% \end{aligned} \quad (3)$$

$$\begin{aligned} \text{the yield of char (wt.\%)} \\ = \frac{m_{\text{solid}} - m_{\text{catalyst}} - m_{\text{unreactedalkalilignin}}}{m_{\text{alkalilignin}}} \times 100\% \end{aligned} \quad (4)$$

$$\begin{aligned} \text{the yield of phenolic products (wt.\%)} \\ = \frac{m_{\text{phenolicproducts}}}{m_{\text{alkalilignin}}} \times 100\% \end{aligned} \quad (5)$$

$m_{\text{bio-oil}}$  is the weight of the bio-oil obtained after the reaction.  $m_{\text{difference}}$  is the weight difference before and after the reaction minus the theoretical mass of CO<sub>2</sub> produced by the decomposition of formic acid,  $m_{\text{alkali lignin}}$  is the total weight of alkali lignin added before the depolymerization reaction,  $m_{\text{unreacted alkali lignin}}$  is the weight of unreacted lignin obtained at the end of the reaction,  $m_{\text{solid}}$  is the weight of the solid obtained after the reaction (including char, catalyst and unreacted lignin),  $m_{\text{catalyst}}$  is the weight of catalyst, and  $m_{\text{phenolic products}}$  is the weight of phenol products (the weight of phenol products was obtained by GC-FID analysis).

**Fig. 2** SEM images of **a** (Ni-W)<sub>10</sub>/ZrP, **b** (Ni-W)<sub>15</sub>/ZrP, **c** (Ni-W)<sub>20</sub>/ZrP, **d** (Ni-W)<sub>25</sub>/ZrP, **e** ZrP, **f** (Ni-W)<sub>20</sub>/ZrP catalyst after 5 cycles, **g** EDX analysis of the catalyst (Ni-W)<sub>20</sub>/ZrP



### 3 Analysis of result

#### 3.1 Catalyst analysis

##### 3.1.1 SEM

To investigate the influence of metal loading on morphology and microstructure of catalyst, catalysts were analyzed across means of SEM, the images are shown in Fig. 2. It can be found that all samples exhibit lamellar stacking structure. From Fig. 2a–e, when the metal loading increases from 10 to 25 wt%, the distribution of active metals on support becomes more uniform. However, the catalyst shows irregular particle structure in the absence of Ni and W rather than the lamellar stacking one. EDX results of (Ni-W)<sub>20</sub>/ZrP catalyst are presented in Fig. 2g and Table 2. It can be found that the element of P and Zr has a higher content (33.12 and 47.87 wt%) and that of Ni and W elements closes to theoretical ratio of 1:1 (9.89 and 9.11 wt%). Figure 2f shows that the catalyst remained intact after five re-uses which indicates that the catalyst has good stability during the alkali lignin depolymerization process.

##### 3.1.2 XRD

Figure 3 shows XRD patterns of (Ni-W)<sub>x</sub>/ZrP catalysts and ZrP support, and ZrP skeletal chain can be observed obviously from all curves. The peaks of nickel oxide (NiO) and tungsten oxide (WO<sub>3</sub>) are not observed by XRD. However, EDX results (see Fig. 2f and Table 2) clearly exhibit the

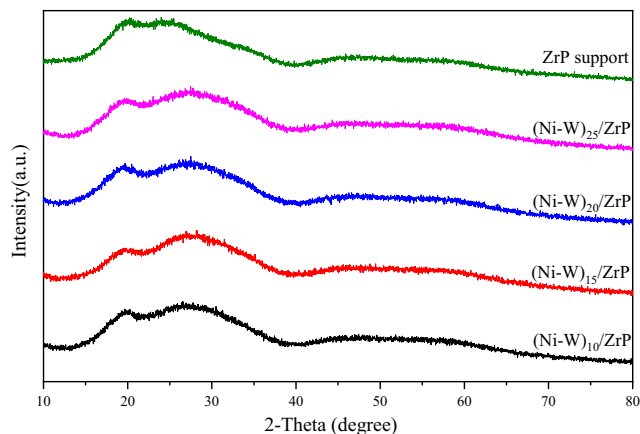


**Fig. 3** XRD patterns of the support and (Ni-W)<sub>x</sub>/ZrP

**Table 3** Physicochemical properties of ZrP support and (Ni-W)<sub>x</sub>/ZrP catalysts

Entry	Sample	Surface area/m <sup>2</sup> g <sup>-1</sup>	Pore volume/cm <sup>3</sup> g <sup>-1</sup>	Pore size/nm
1	(Ni-W) <sub>10</sub> /ZrP	40.87	0.06	5.77
2	(Ni-W) <sub>15</sub> /ZrP	37.75	0.05	5.64
3	(Ni-W) <sub>20</sub> /ZrP	36.48	0.05	5.93
4	(Ni-W) <sub>25</sub> /ZrP	33.00	0.04	5.87
5	ZrP	85.80	0.10	5.30

content of Ni and W elements, which indicates that Ni and W metal are evenly dispersed on the surface of ZrP support or are possibly formed as the metal alloy (Ni-W-Zr/O<sub>x</sub>).

### 3.1.3 BET

N<sub>2</sub> adsorption–desorption isotherms of catalysts and support are shown in Fig. 4. All isotherms show a clear type IV pattern, with the ordered nature of the mesopores illustrated by the H3 lag loop at P/P<sub>0</sub> of 0.6–1.0 [33–35]. Table 3 gives the physicochemical properties of (Ni-W)<sub>x</sub>/ZrP and ZrP. ZrP support shows the highest surface area of 85.8 m<sup>2</sup> g<sup>-1</sup>, while the surface area and pore volume tend to decrease with the increasing of metal loading, which is due to the pore blockage. As shown in Fig. 4b, the pore volume tends to decrease with increasing Ni, W metal loading compared to the support, which follows the same trend as the pore volume (BJH method) distribution given in Table 3. All catalysts have small pore sizes (5–6 nm), indicating that metals of Ni, W are uniformly dispersed on the support and can participate in lignin depolymerization efficiently.

## 3.2 Effects of reaction parameters

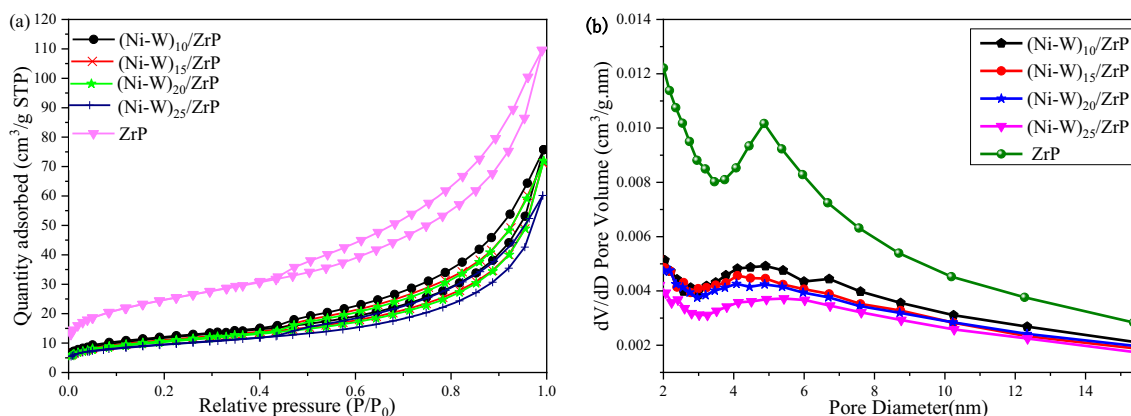
### 3.2.1 Effects of FA and catalyst additions on lignin depolymerization

Figure 5 shows effects of catalyst and formic acid (FA) additions on depolymerization of alkali lignin. The highest yield of

unreacted alkali lignin (60.30 wt%), and the lowest bio-oil yield (17.85 wt%) are all obtained at NON. The yield of bio-oil increases as adding the catalyst (Ni-W)<sub>20</sub>/ZrP or FA, which can be explained that the catalyst (Ni-W)<sub>20</sub>/ZrP inhibits the formation of char to a certain extent. However, as only adding FA, the char yield increases significantly from 11.23 to 47.30 wt%, which demonstrates that FA is favorable for alkali lignin depolymerization but also plays a role in promoting the formation of char. However, the yield of bio-oil is as high as 74.66 wt% and the char yield is significantly low (only 11.23 wt%) with the synergistic effect of FA and catalyst. It is suggested that FA can act as a good hydrogen donor to assist the catalyst on alkali lignin depolymerization.

### 3.2.2 Effect of reaction temperature on alkali lignin depolymerization

Figure 6 shows the effect of reaction temperature (180–240 °C) on alkali lignin depolymerization with the metal loading of 20 wt% (Ni, W). The yield of bio-oil increases from 43.10 to 74.66 wt% as temperature increases from 180 to 240 °C, which can be instructed that the depolymerization of alkali lignin is a heat absorption reaction [32]. When the reaction temperature increases from 180 to 220 °C, the yield of char decreases from 25.68 to 11.23 wt%. Figure 5 illustrates that when only FA was added, the char yield is high, so at low temperature, the char yield is high which could be explained by the FA mainly acting as acid catalyst instead of hydrogen donor. Higher temperature seems to be required to activate the



**Fig. 4** a N<sub>2</sub>-adsorption and desorption isotherm. b Pore size distribution of catalysts

dehydrogenation of the FA. When the temperature was increased, the yield of unreacted lignin also showed a decreasing trend, which can further indicate that higher temperature can promote the depolymerization of alkali lignin. However, the char yield does not further reduce by continuously increasing the temperature. Because at high temperature range, the repolymerization of monomers occurs, which will accelerate char formation [36, 37].

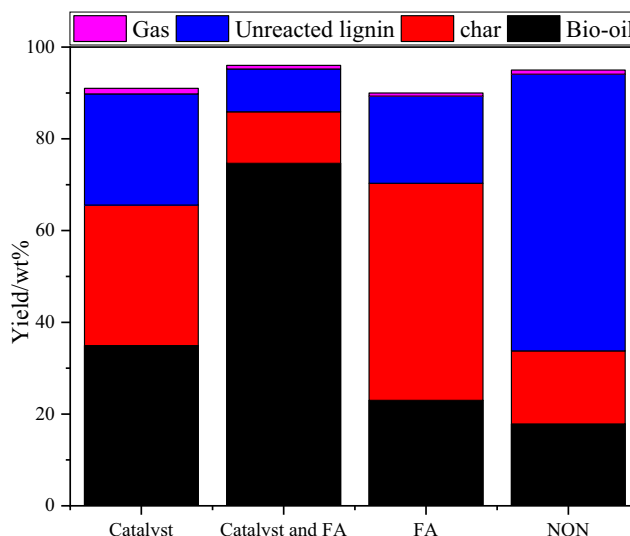
### 3.2.3 Effects of Ni, W loadings on lignin depolymerization

Figures 7 a and b show the effect of Ni and W loadings on alkali lignin depolymerization. From Fig. 7a, the highest conversion rate of alkali lignin is 74.66 wt% as the active metal loading is 20 wt%. No obvious increase occurs in lignin conversion when the metal loading continuously increases, which is because the excessive loading of active metal will lead to the excessive hydrogenolysis of lignin [38]. From Fig. 7b, further analysis of GC-MS shows that, when the metal loading is 25 wt%, the relative content of phenolic monomers decreases significantly from 88.25 to 74.69 wt%, and that of aliphatic compounds (shown in Table 4) which are mainly generated by esterification, etherification, dehydration condensation reaction between formic acid and depolymerization product or between solvent molecules, increases significantly from 11.75 to 25.31 wt%. In particular, over (Ni-W)<sub>10</sub>/ZrP catalyst, only 56.68 wt% of alkali lignin was converted to product (bio-oil) due to the limited number of active metal centers (Ni and W).

## 3.3 Product analysis

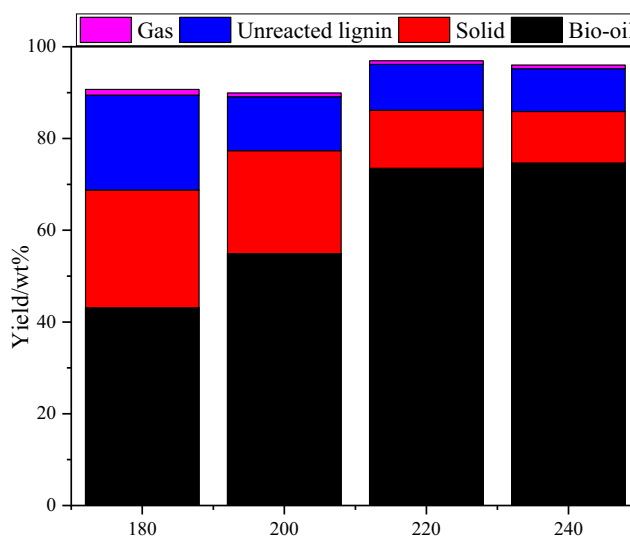
### 3.3.1 GC/MS analysis of bio-oil

GC/MS analysis was applied to analyze the substances in bio-oil. From Fig. 8a, the relative content (%) of phenols obtained is based on all substances detected in bio-oil, including ketones, ethers, lipids, and phenolic components, by the normalization of peak area. Figure 8 b, c, and d show the relative content of phenolic monomers on the base of all phenols (including G-, H-, and S-types) by the normalization of peak area. Table 5 shows the information of the main G-phenolic products in the bio-oil which was obtained under different reaction conditions. Figure 8a shows the relative content of total phenols G-phenols obtained at different temperatures differs very little, indicating that the catalyst (Ni-W)<sub>20</sub>/ZrP has excellent selectivity for G-phenolic products. The total relative content of phenolic substances declines from 88.54 to 80.79% as the temperature increases from 180 to 240 °C. It demonstrates that high temperatures have an active effect on the yield of bio-oil, but there is a negative effect on the selectivity of phenolic substances. At high temperatures, phenolic monomers produced have undergone further hydrolysis, and some aliphatic compounds (ethers, lipids, etc.) have been generated through a series of hydrolysis,



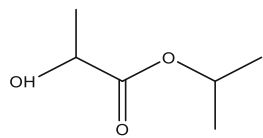
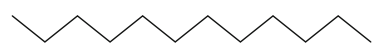
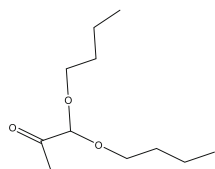
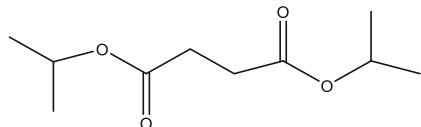
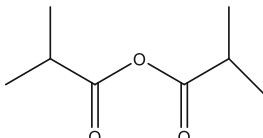

**Fig. 5** Effects of catalyst and FA additions on the depolymerization of alkali lignin. (Catalyst: only 0.2 g catalyst (Ni-W)<sub>20</sub>/ZrP is added. Catalyst and FA: 0.2 g Ni-W<sub>20</sub>/ZrP catalyst and 5 mL formic acid are added. FA: only 5 mL FA is added. NON: neither catalyst nor FA is added.) Common conditions: lignin 0.5 g, isopropanol 50 mL

hydrogenation, and polymerization. Figure 8b shows the selectivity of vanillin in bio-oil at different reaction temperatures. Vanillin is used in cosmetics, tobacco, and food industries, as a growth promoter of plants, fungicides, etc., and can be used as an important intermediate in the manufacture of medicines and other spices. The relative content of vanillin (G7) decreases from 45.59 to 8.55% as the temperature increases from 180 to 240 °C, which can be explained by the fact that low temperature favors the selectivity conversion of alkali lignin to vanillin. The selectivity to alkyl G-type phenols (G1, G2, G3, G4, G5, G6, and G8) tended to increase with increasing temperature (from 18.65% to 58.47%). Some phenolic monomer products with



**Fig. 6** Effect of reaction temperature on alkali lignin depolymerization. Common conditions: 0.5 g alkali lignin; 0.1 g Ni-W<sub>20</sub>/ZrP catalyst; 50 mL isopropanol; 5 mL FA

**Table 4** Information on the main aliphatic compounds in bio-oil

No.	RT (min)	Aliphatic Compound	Compound Structure
1	6.62	(S)-Isopropyl lactate	
2	9.62	Dodecane	
3	10.24	2-Propanone, 1,1-dibutoxy-	
4	10.34	Succinic acid diisopropyl ester	
5	11.71	Propanoic acid, 2-methyl-, anhydride	
6	18.69	n-Hexadecanoic acid	

oxygen (G9~G18), which can be reprocessed and reused for high value-added chemicals such as petroleum energy. Figure 8c shows that when formic acid and catalyst are added at the same time, the types of phenolic monomers in bio-oil are more abundant, which indicates that formic acid and catalyst have a good synergistic effect on the selective depolymerization process of alkali lignin.

### 3.3.2 GC-FID analysis of bio-oil

Figure 9 shows the quantitative yields of the main phenolic products in the bio-oil obtained during the depolymerization of alkali lignin by the catalyst at different reaction temperatures. Four main phenolic products with high content in bio-oil are phenol,2-methoxy-, phenol,4-ethyl-2-methoxy,

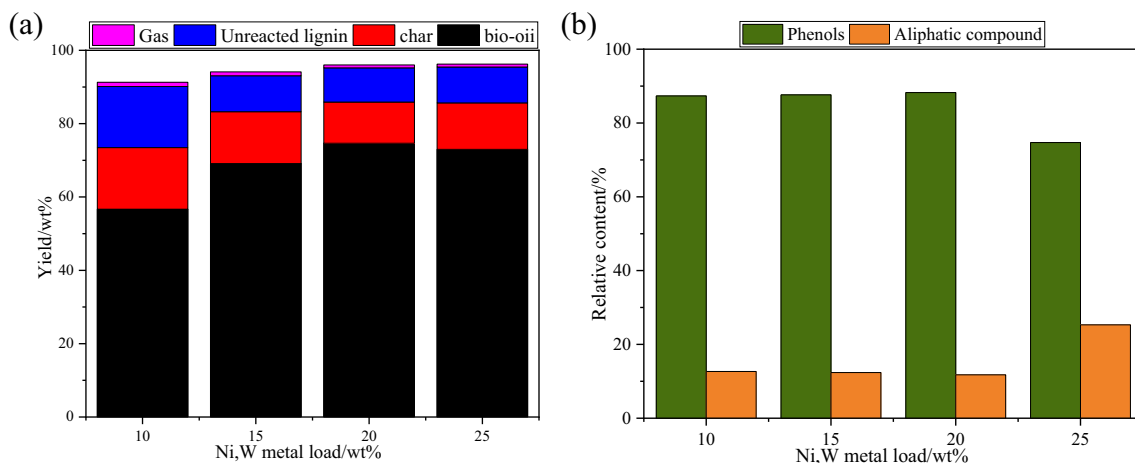


**Fig. 7** Effect of Ni and W loading on hydrogenolysis of alkali lignin. Common conditions: reaction temperature: 240 °C; reaction time: 8 h; alkali lignin: 0.5 g; catalyst addition: 0.1 g; formic acid addition: 5 mL; isopropanol 50 mL

**Table 5** Information on G-type phenols in bio-oil under different reaction conditions

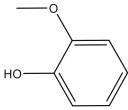
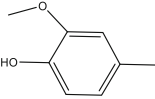
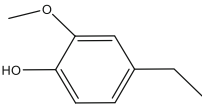
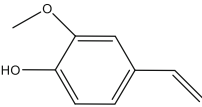
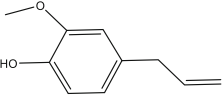
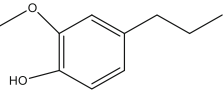
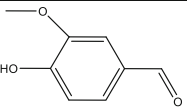
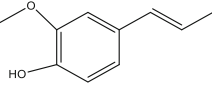
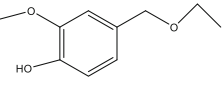
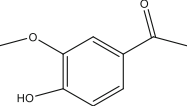
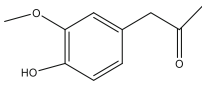
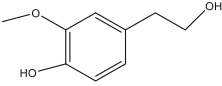
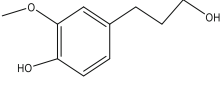
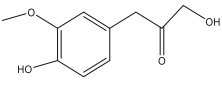
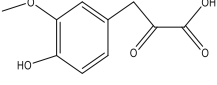
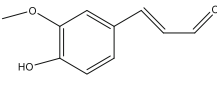
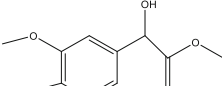
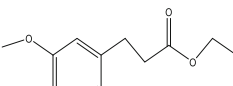
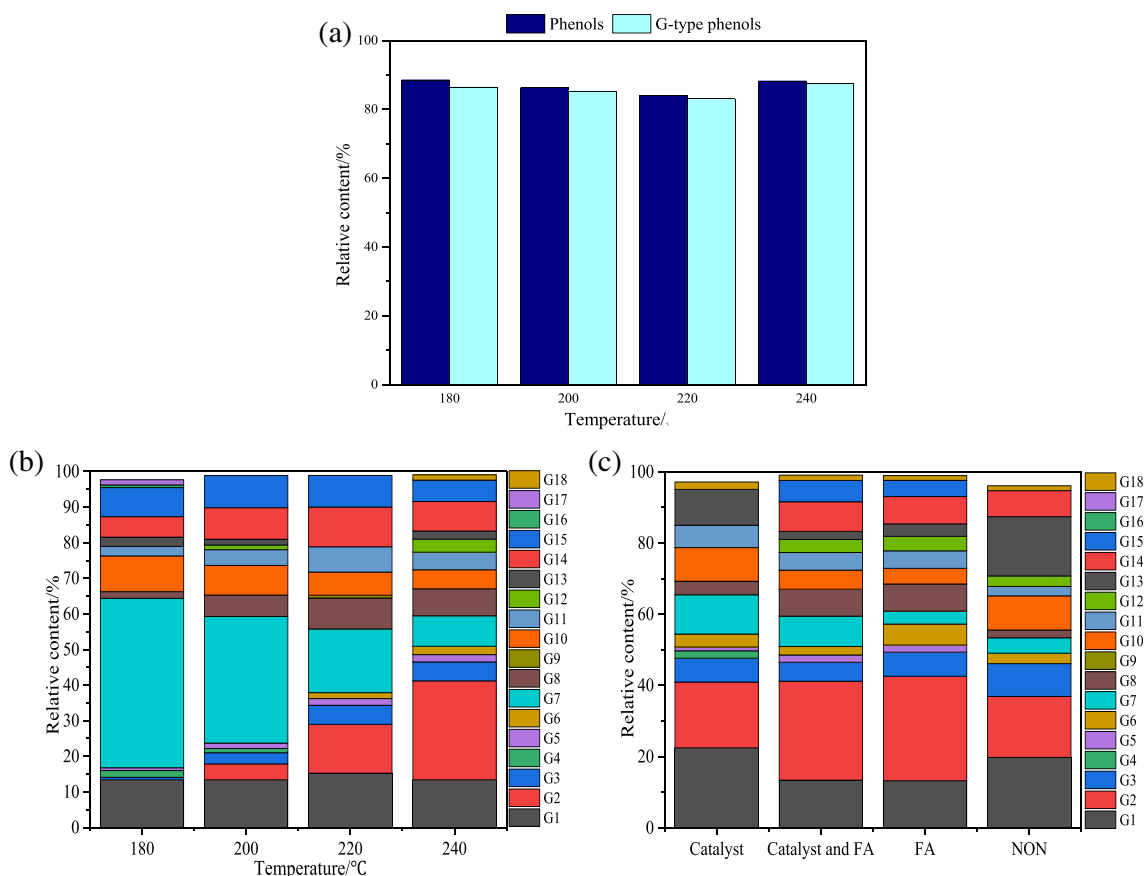
No.	RT (min)	Compound	Compound Structure	Area (%)						
				180°C	200°C	220°C	240°C	Cat.	FA	NON
G1	8.15	Phenol,2-met hoxy-		9.17	8.31	9.23	9.00	15.99	9.23	14.1
G2	9.68	Creosol		-	2.76	8.29	18.67	13.17	20.5	12.25
G3	10.90	Phenol, 4-ethyl-2-met hoxy-		0.49	1.94	3.23	3.59	4.78	4.72	6.57
G4	11.40	2-Methoxy-4 -vinylphenol		11.40	0.75	-	-	1.42	-	-
G5	11.97	Eugenol		0.84	0.94	1.14	1.37	0.75	1.37	-
G6	12.09	Phenol,2-met hoxy-4-propy l-		-	-	1.00	1.59	0.65	2.59	0.97
G7	12.61	Vanillin		32.61	22.02	10.82	5.75	7.84	2.54	3.08
G8	13.18	Phenol,2-met hoxy-4-(1pro penyl)-, (E)-		1.29	3.73	5.26	5.08	2.72	5.33	1.57
G9	13.33	Phenol,4-(eth oxymethyl)-2- methoxy-		-	-	0.47	-	-	-	-
G10	13.71	Ethanone,1-( 4-hydroxy-3- methox -henyl)-		6.86	5.18	3.93	3.60	6.73	3.05	6.84



Table 5 (continue)

G11	14.22	2-Propanone, 1-(4-hydroxy-3-methoxyphenyl)-		1.86	2.73	4.29	2.44	4.47	2.07	1.89
G12	14.28	Homovanillyl alcohol		-	0.82	-	2.45	-	2.86	2.09
G13	15.64	Benzenepropanol, 4-hydroxy-3-methoxy-		1.75	0.99	-	1.54	7.16	1.67	6.23
G14	15.73	2-Propanone, 1-hydroxy-3-(4-hydroxy-3-methoxyphenyl)-		3.96	5.49	6.75	5.57	-	5.35	5.23
G15	16.61	Phenylacetic acid, 4-hydroxy-3-methoxy-		5.58	5.59	5.37	4.04	-	3.19	-
G16	16.72	Coniferyl aldehyde		0.52	-	-	-	-	-	-
G17	16.94	Benzeneacetic acid, 4-hydroxy-3-methoxy-, methyl ester		0.98	-	-	-	-	-	-
G18	16.97	Ethyl 4-(4-hydroxy-3-methoxyphenyl)-propionate		-	-	-	1.00	1.48	0.92	0.97



**Fig. 8** a Effect of reaction temperature on the selective conversion of alkali lignin to phenol products (including G-, H- and S-type phenols, relative content, %). b Effect of reaction temperature on the selective

conversion of alkali lignin to G-type phenols (relative content, %). c Effect of catalyst and FA additions on the selective conversion of alkali lignin to G-type phenols (relative content, %)

vanillin, and ethanone,1-(4-hydroxy-3-methoxy-henyl) which can be used as edible spice and medicinal herbs in the industrial production. Figure 9 shows that temperature has a greater influence on the content of the phenolic products. When the reaction temperature is 240 °C, the total content of phenolic

monomers is at a minimum (2.77 wt%), which can be explained by further reactions (repolymerization) of the phenolic monomers at higher temperatures leading to the formation of dimer.

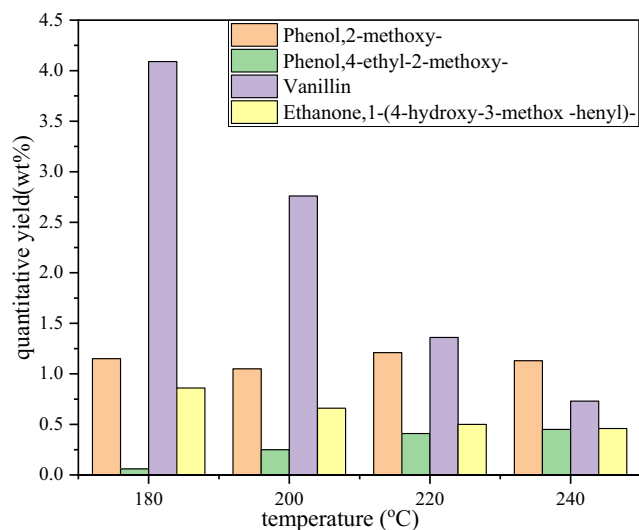


**Fig. 9** The mass of main phenolic products at different temperatures

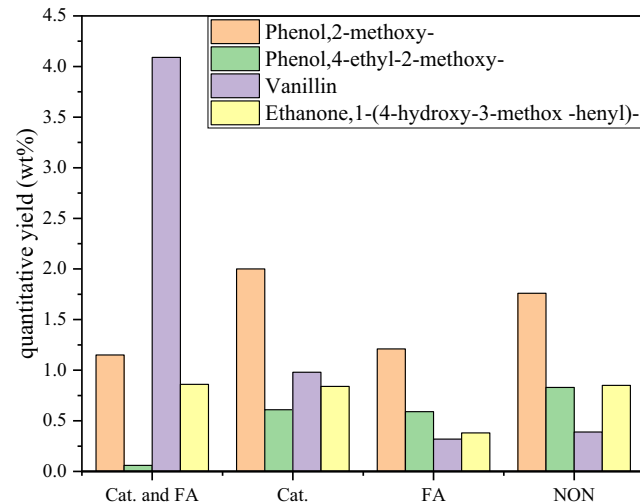


**Fig. 10** The mass of main phenolic products under different reaction conditions

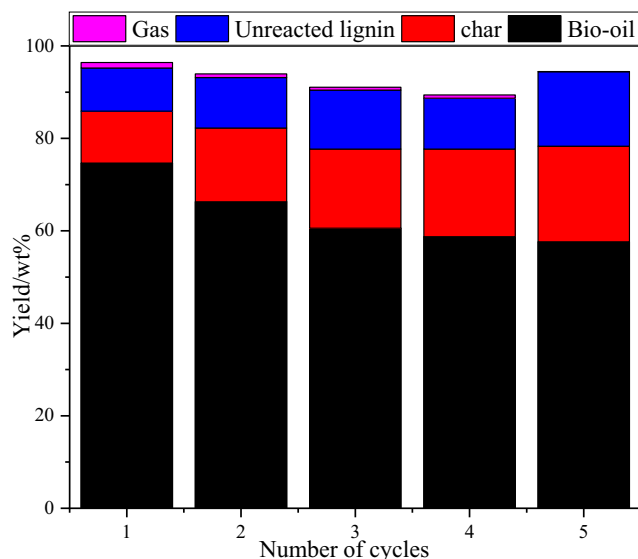
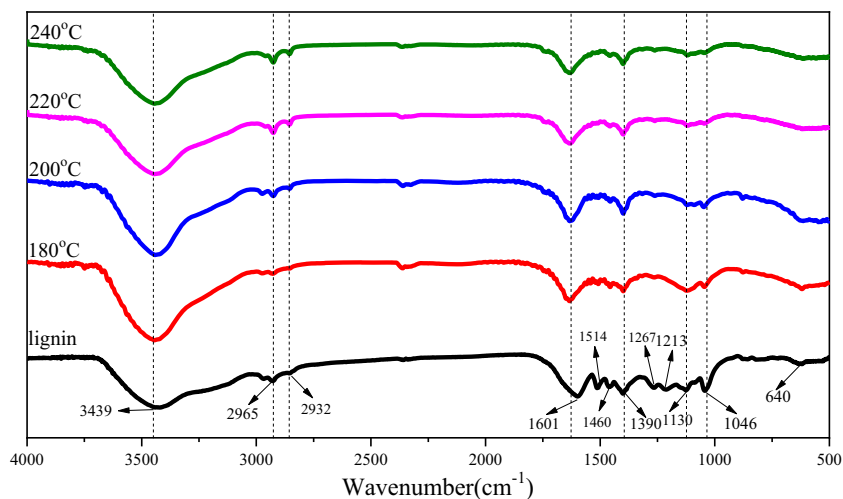


**Fig. 11** Reusability test of (Ni-W)<sub>20</sub>/ZrP catalyst for alkali lignin depolymerization at 240 °C for 8 h

Figure 10 shows the mass of main phenolic products under different reaction conditions. When only catalyst was added, the total phenolic product content was 4.43 wt%; however, when only formic acid was added, the phenolic product content was reduced to 2.5 wt%, indicating that the (Ni-W)<sub>20</sub>/ZrP shows excellent ability for hydrogenolysis of ether bonds in alkali lignin and performed relatively well in the depolymerization of alkali lignin. The total content (6.16 wt%) of phenol products in bio-oil was much higher when formic acid and catalyst acted synergistically than when only formic acid or only catalyst was added during the depolymerization of alkali lignin. It can be explained that formic acid can assist the catalyst of (Ni-W)<sub>20</sub>/ZrP in the depolymerization of alkali lignin with excellent performance.

Related reports [39–41] also indicate that in the depolymerization process of alkali lignin with formic acid or related catalysts, the yield of phenolic products is highly dependent on reaction conditions such as temperature and pressure.

**Fig. 12** FTIR spectra of original lignin and unreacted lignin after depolymerization



However, although the yield of bio-oil has been improved in this study, the yields of bio-oil are mostly inferior aromatic products, and the yield of phenolic products was very low, generally not exceeding 6 wt%. The total yield of phenolic products obtained in this study is not less than 6.16 wt%, which further illustrates the effectiveness and high selectivity of the prepared catalyst of (Ni-W)<sub>20</sub>/ZrP.

### 3.4 Reusability of catalyst

The stability of synthetic catalyst is an important index to show whether the catalyst can be used effectively. In this study, the stability of the catalyst was investigated by using the catalyst separated from the first experiment in the cycle experiment. From Fig. 11, it can be seen that after five cycles, the catalyst performance was almost stable. The yield of bio-oil decreased from 77.46% to 57.64 wt% and then gradually stabilized.

### 3.5 Analysis of unreacted lignin

FTIR results of alkali lignin and unreacted lignin are shown in Fig. 12, in which the FT-IR spectrum is allocated by referring to references [42, 43]. The spectra of lignin and unreacted lignin are similar, indicating that their functional groups are similar. FT-IR results of the original lignin showed a broad absorption peak at 3439 cm<sup>-1</sup> due to the stretching effect of the -OH groups. Vibrations located at 2965 cm<sup>-1</sup> and 2932 cm<sup>-1</sup> are derived from methyl and methylene C-H bonds. Vibrations located at 1601 cm<sup>-1</sup>, 1514 cm<sup>-1</sup>, and 1460 cm<sup>-1</sup> and 650 cm<sup>-1</sup> are attributed to aromatic ring. In addition, peak at 1390 cm<sup>-1</sup> finds the C-H symmetric deformation band in methoxy-CH<sub>3</sub>. Finally, the peaks of 1267 cm<sup>-1</sup>, 1213 cm<sup>-1</sup>, 1130 cm<sup>-1</sup>, and 1046 cm<sup>-1</sup> are derived from vibrating of the C-O bond in the guaiac-based and clove-based units.

The absorbance of functional groups in unreacted lignin decreases with increasing temperature compared to pristine lignin. When the reaction temperature increases to 240 °C, the signal of -OH stretching decreases which presents the disappearance of hydroxyl groups in lignin structure. In particular, peaks at 1267 cm<sup>-1</sup>, 1213 cm<sup>-1</sup>, 1130 cm<sup>-1</sup>, and 1046 cm<sup>-1</sup> (C-O bonds in guaiac-based and clove-based units) gradually decrease with the increase of temperature which indicates that lignin is depolymerized to monoaromatic units effectively.

## 4 Conclusions

Ni-W<sub>x</sub>/ZrP catalysts prepared by chemical reduction provided effectively catalytic activity in lignin depolymerization. The highest catalytic effect was achieved when the ZrP support is loaded with Ni, W at 20 wt%. Excessive loading could lead to excessive hydrogenolysis of lignin and increase the char yield. The reaction temperature was the key factor on generation of phenolic products. High temperatures favored lignin conversion but were not beneficial for the creation of phenolic monomers. Effect of temperature on the selectivity to vanillin was evident, with the highest proportion at 180 °C (45.59%, relative content). Additionally, increasing temperature favored selectivity of lignin to G-type alkylphenols. Formic acid and catalyst play an excellent synergistic role in the depolymerization of lignin, with the highest content of phenolic products (6.16 wt%). FTIR analysis of original alkali lignin and unreacted lignin showed that lignin was efficiently converted into phenolics via hydrogenolysis.

**Author contribution** D.W. and X.L. contributed equally. Conceptualization, D.W.; methodology, X.L.; software, P.X.; validation, H.G., J.C., and Y.Q.; formal analysis, C.X.; investigation, X.G.; resources, X.G. and X.L.; data curation, D.W.; writing—original draft preparation, D.W.; writing—review and editing, X.G. and X.L.; visualization, H.M.R.; supervision, X.G.; project administration, C.X.; funding acquisition, X.G. All authors have read and agreed to the published version of the manuscript.

**Funding** This research was financially supported by National Natural Science Foundation of China (No.21774059), the Priority Academic Program Development (PAPD) of Jiangsu Higher Education Institutions, and the opening funding of Jiangsu Key Lab of Biomass based Green Fuels and Chemicals.

## Declaration

**Competing interests** The authors declare no competing interests.

## References

- Beauchet R, Monteil-Rivera F, Lavoie JM (2012) Conversion of lignin to aromatic-based chemicals (*L*-chems) and biofuels (*L*-fuels). *Bioresour Technol* 121:328–334. <https://doi.org/10.1016/j.biortech.2012.06.061>
- Guan W, Tsang CW, Lin CSK, Len C, Liang C (2019) A review on high catalytic efficiency of solid acid catalysts for lignin valorization. *Bioresour Technol* 298:122432. <https://doi.org/10.1016/j.biortech.2019.122432>
- Ferrini P, Rinaldi R (2014) Catalytic biorefining of plant biomass to non-pyrolytic lignin bio-oil and carbohydrates through hydrogen transfer reactions. *Angew Chem Int Ed* 53:8634–8639. <https://doi.org/10.1002/anie.201403747>
- Tymchyshyn M, Yuan Z, Zhang Y, Xu CC (2019) Catalytic hydrodeoxygenation of guaiacol for organosolv lignin depolymerization-catalyst screening and experimental validation. *Fuel* 254:115664. <https://doi.org/10.1016/j.fuel.2019.115664>
- Zaheer M, Kempe R (2015) Catalytic hydrogenolysis of aryl ethers: a key step in lignin valorization to valuable chemicals. *ACS Catal* 5: 1675–1684. <https://doi.org/10.1021/cs501498f>
- Farag S, Mudraboyina BP, Jessop PG, Chaouki J (2016) Impact of the heating mechanism on the yield and composition of bio-oil from pyrolysis of kraft lignin. *Biomass Bioenergy* 95:344–353. <https://doi.org/10.1016/j.biombioe.2016.07.005>
- Zhu X, Lobban LL, Mallinson RG, Resasco DE (2011) Bifunctional transalkylation and hydrodeoxygenation of anisole over a Pt/H Beta catalyst. *J Catal* 281:21–29. <https://doi.org/10.1016/j.jcat.2011.03.030>
- Parsell TH, Owen BC, Klein I, Jarrell TM, Abu-Omar MM (2013) Cleavage and hydrodeoxygenation (HDO) of C-O bonds relevant to lignin conversion using Pd/Zn synergistic catalysis. *Chem Sci* 4: 806–813. <https://doi.org/10.1039/C2SC21657D>
- Zheng, Shuang, El-Shall M, Samy, Zhong, Lin YJ, Andrew, Zhang (2016) Synergetic catalysis of palladium nanoparticles encaged within amine-functionalized UiO-66 in the hydrodeoxygenation of vanillin in water. *Green Chem* 18:2900–2908. <https://doi.org/10.1039/c5gc02615f>
- Lee SH, Doherty TV, Linhardt RJ, Dordick JS (2009) Ionic liquid-mediated selective extraction of lignin from wood leading to enhanced enzymatic cellulose hydrolysis. *Biotechnol Bioeng* 102: 1368–1376. <https://doi.org/10.1002/bit.22179>
- Li S, Luo Z, Wang W, Sun H, Liang X (2020) Catalytic fast pyrolysis of enzymatic hydrolysis lignin over Lewis-acid catalyst niobium pentoxide and mechanism study. *Bioresour Technol* 316: 123853. <https://doi.org/10.1016/j.biortech.2020.123853>
- Naicker JE, Govinden R, Lekha P, Sithole B (2020) Transformation of pulp and paper mill sludge (PPMS) into a glucose-rich hydrolysate using green chemistry: assessing pretreatment methods for enhanced hydrolysis. *J Environ Manag* 270:110914. <https://doi.org/10.1016/j.jenvman.2020.110914>
- Luo Z, Zheng Z, Wang Y, Sun G, Jiang H, Zhao C (2016) Hydrothermally stable Ru/HZSM-5-catalyzed selective hydrogenolysis of lignin-derived substituted phenols to bio-arenes in water. *Green Chem* 18:5845–5858. <https://doi.org/10.1039/C6GC01971D>
- Forberg D, Schwob T, Zaheer M, Friedrich M, Miyajima N, Kempe R (2016) Single-catalyst high-weight% hydrogen storage in an N-heterocycle synthesized from lignin hydrogenolysis products and ammonia. *Nat. Commun.* 7:13201. <https://doi.org/10.1038/ncomms13201>
- Lin B, Li R, Shu R, Wang C, Chen Y (2020) Hydrogenolysis and hydrodeoxygenation of lignin in a two-step process to produce hydrocarbons and alkylphenols. *J Energy Inst* 93:784–791. <https://doi.org/10.1016/j.joei.2019.05.004>
- Feng X, Simpson AJ, Wilson KP, Dudley Williams D, Simpson MJ (2008) Increased cuticular carbon sequestration and lignin oxidation in response to soilwarming. *Nat Geosci* 1:836–839. <https://doi.org/10.1038/ngeo361>

17. Zhou G, Li J, Chen Y, Zhao B, Cao Y, Duan X, Cao Y (2009) Determination of reactive oxygen species generated in laccase catalyzed oxidation of wood fibers from Chinese fir (*Cunninghamia lanceolata*) by electron spin resonance spectrometry. *Bioresour Technol* 100:505–508. <https://doi.org/10.1016/j.biortech.2008.06.010>
18. Davaritouchaee M, Hiscox WC, Terrell E, Mancini RJ, Chen S (2020) Mechanistic studies of milled and Kraft lignin oxidation by radical species. *Green Chem* 22:1182–1197. <https://doi.org/10.1039/C9GC04162A>
19. Totong S, Daorattanachai P, Laosiripojana N, Idem R (2020) Catalytic depolymerization of alkali lignin to value-added phenolic-based compounds over Ni/CeO<sub>2</sub>-ZrO<sub>2</sub> catalyst synthesized with a one-step chemical reduction of Ni species using NaBH<sub>4</sub> as the reducing agent. *Fuel Process Technol* 198:13. <https://doi.org/10.1016/j.fuproc.2019.106248>
20. Salakhum S, Saenluang K, Wattanakit C (2020) Stability of monometallic Pt and Ru supported on hierarchical HZSM-5 nanosheets for hydrodeoxygenation of lignin-derived compounds in the aqueous phase. *Sustain Energy Fuels* 4:1126–1134. <https://doi.org/10.1039/C9SE00773C>
21. Hao N, Alper K, Patel H, Tekin K, Ragauskas AJ (2020) One-step transformation of biomass to fuel precursors using a bi-functional combination of Pd/C and water tolerant Lewis acid. *Fuel* 277:118200. <https://doi.org/10.1016/j.fuel.2020.118200>
22. Parto SG, Jørgensen EK, Christensen JM, Pedersen LS, Larsen DB, Duus JØ, Jensen AD (2020) Solvent assisted catalytic conversion of beech wood and organosolv lignin over NiMo/γ-Al<sub>2</sub>O<sub>3</sub>. *Sustain Energy Fuels* 4:1844–1854. <https://doi.org/10.1039/C9SE00375D>
23. Guo H, Li C, Qi Z, Liu Y, Xia H, Li L, Huang Q, Wang AQ (2019) Tungsten-based catalysts for lignin depolymerization: the role of tungsten species in C–O bond cleavage. *Catal Sci Technol* 9:2144–2151. <https://doi.org/10.1039/C9CY00251K>
24. Fan XD, Wu YJ, Li ZY, Sun Y, Tu R, Zhong PD, Jiang EC, Xu XW (2020) Benzene, toluene and xylene (BTX) from in-situ gas phase hydrodeoxygenation of guaiacol with liquid hydrogen donor over bifunctional non-noble-metal zeolite catalysts. *Renew Energy* 152:1391–1402. <https://doi.org/10.1016/j.renene.2020.01.015>
25. Ochoa A, Aramburu B, Valle B, Resasco D, Bilbao J, Gayubo AG (2017) Role of oxygenates and effect of operating conditions in the deactivation of a Ni supported catalyst during the steam reforming of bio-oil. *Green Chem* 19:4315–4333. <https://doi.org/10.1039/C7GC01432E>
26. Song Q, Wang F, Cai J, Wang Y, Zhang J, Yu W, Xu J (2013) Lignin depolymerization (LDP) in alcohol over nickel-based catalysts via a fragmentation–hydrogenolysis process. *Energy Environ Sci* 6:994–1007. <https://doi.org/10.1039/c2ee23741e>
27. Song W, Lai W, Lian Y, Jiang X, Yang W (2019) Sulfated ZrO<sub>2</sub> supported CoMo sulfide catalyst by surface exsolution for enhanced hydrodeoxygenation of lignin-derived ethers to aromatics. *Fuel* 263:116705. <https://doi.org/10.1016/j.fuel.2019.116705>
28. Weingarten R, Kim YT, Tompsett GA, Fernández A, Huber GW (2013) Conversion of glucose into levulinic acid with solid metal (IV) phosphate catalysts. *J Catal* 304:123–134. <https://doi.org/10.1016/j.jcat.2013.03.023>
29. Rao KN, Sridhar A, Lee AF, Tavener SJ, Young NA, Wilson K (2006) Zirconium phosphate supported tungsten oxide solid acid catalysts for the esterification of palmitic acid. *Green Chem* 8:790–797. <https://doi.org/10.1039/B606088A>
30. Ma H, Li H, Zhao W, Li L, Liu S, Long J, Li X (2019) Selective depolymerization of lignin catalyzed by nickel supported on zirconium phosphate. *Green Chem* 21:658–668. <https://doi.org/10.1039/C8GC03617A>
31. Han GH, Lee MW, Park S, Kim HJ, Ahn JP, Seo MG, Lee KY (2019) Revealing the factors determining the selectivity of guaiacol HDO reaction pathways using ZrP-supported Co and Ni catalysts. *J Catal* 377:343–357. <https://doi.org/10.1016/j.jcat.2019.07.034>
32. Lu X, Zhu X, Guo H, Que H, Gu X (2020) Efficient depolymerization of alkaline lignin to phenolic compounds at low temperatures with formic acid over inexpensive Fe-Zn/Al<sub>2</sub>O<sub>3</sub> catalyst. *Energy Fuel* 34:7121–7130. <https://doi.org/10.1021/acs.energyfuels.0c00742>
33. Santhana Krishnan P, Ramya R, Umasankar S, Shanthi K (2017) Promotional effect of Ni<sub>2</sub>P on mixed and separated phase MoS<sub>2</sub>/Al-SBA-15 (10) catalyst for hydrodenitrogenation of ortho-Propylaniline. *Microporous Mesoporous Mater* 242:208–220. <https://doi.org/10.1016/j.micromeso.2017.01.031>
34. Chun H, Wang MH, Naghadeh S, Bonabi JZ, Zhong, Fang FP (2018) Visible light driven hydrogen evolution by photocatalytic reforming of lignin and lactic acid using one-dimensional NiS/CdS nanostructures. *Appl Catal B-Environ* 227:229–239. <https://doi.org/10.1016/j.apcatb.2018.01.038>
35. Xu J, Li M, Yang L, Qiu J, Yao J (2020) Synergy of Ni dopant and oxygen vacancies in ZnO for efficient photocatalytic depolymerization of sodium lignosulfonate. *Chem Eng J* 394:125050. <https://doi.org/10.1016/j.cej.2020.125050>
36. Long JX, Xu Y, Wang TJ, Yuan ZQ, Shu RY, Zhang Q, Ma L (2015) Efficient base-catalyzed decomposition and in situ hydrogenolysis process for lignin depolymerization and char elimination. *Appl Energy* 141:70–79. <https://doi.org/10.1016/j.apenergy.2014.12.025>
37. Si XQ, Chen JZ, Lu F, Liu XY, Ren YJ, Lu R, Jiang HF, Liu H, Miao S, Zhu Y, Luo XL, Xu J (2019) Immobilized Ni clusters in mesoporous aluminum silica nanospheres for catalytic hydrogenolysis of lignin. *ACS Sustain Chem Eng* 7:19034–19041. <https://doi.org/10.1021/acssuschemeng.9b04746>
38. Li H, Ma H, Zhao W, Li X, Long J (2019) Upgrading lignin bio-oil for oxygen-containing fuel production using Ni/MgO: Effect of the catalyst calcination temperature. *Appl Energy* 253:12. <https://doi.org/10.1016/j.apenergy.2019.113613>
39. Singh SK, Dhepe PL (2020) Formic-acid-induced using recyclable ionic liquids as catalysts for lignin conversion into aromatic co-products. *Waste Biomass Valorization* 11:6261–6272. <https://doi.org/10.1007/s12649-019-00896-3>
40. Zhang ZS, Du BY, Zhu HW, Chen CZ, Sun Y, Wang X, Zhou JH, Facile adjusting the concentration of siliceous seed to obtain different HZSM-5 zeolite catalysts for effective catalytic depolymerization reaction of lignin, *Biomass Convers. Biorefinery*, 12. <https://doi.org/10.1007/s13399-021-01352-w>
41. Hong-Xia F, Peng C, Chen Q (2021) Behavior characterization of lignosulfonate depolymerization products under acid-catalyzed conditions using gas chromatography-mass spectrometry. *Chromatographia* 84:109–116. <https://doi.org/10.1007/s10337-020-03988-8>
42. Faix O (1991) Classification of lignins from different botanical origins by FT-IR spectroscopy. *Holzforschung* 45:21–28. <https://doi.org/10.1515/hfsg.1991.45.s1.21>
43. Wen JL, Sun SL, Yuan TQ, Xu F, Sun R-C (2014) Understanding the chemical and structural transformations of lignin macromolecule during torrefaction. *Appl Energy* 121:1–9. <https://doi.org/10.1016/j.apenergy.2014.02.001>